APPLIED AND ENVIRONMENTAL MICROBIOLOGY, Mar. 1996, p. 1029–1035 Vol. 62, No. 3
0099-2240/96/$04.00+0

A Combined Model for Growth and Subsequent Thermal Inactivation of *Brochothrix thermosphacta*

J. BARANYI,* A. JONES, C. WALKER, A. KALOTI, T. P. ROBINSON, AND B. M. MACKEY

Institute of Food Research, Reading Laboratory, Reading RG6 6BZ, United Kingdom

Received 24 July 1995/Accepted 21 December 1995

A mathematical technique for integrating growth and thermal inactivation models of microorganisms into a smooth combined model that can be applied to circumstances under which the temperature gradually rises from growth to inactivation regions is described. For the death part of the model, a correction term is introduced to allow for additional resistance of the cells gained during slow heating. The model was validated with *Brochothrix thermosphacta* heated in broth at rising temperatures.

A large number of prepared food products that depend for their safety on a mild heat treatment combined with refrigerated storage are now available. These include refrigerated foods of extended durability that may have a shelf life of between 3 and 6 weeks and cook-chill, "sous-vide," or other types of prepared meals that are stored for shorter periods. The recommended heat treatments and storage temperatures depend on the type of product and its intended shelf life (reviewed in reference 14), but they are designed to eliminate and/or prevent growth of vegetative pathogens such as *Listeria monocytogenes* and spore-forming nonproteolytic *Clostridium botulinum* organisms.

There is a continuing trend towards minimal processing, to ensure retention of flavor, texture, and aroma, and some recommended heat processes would reduce numbers of *L. monocytogenes* by only four $\log_{10}$ units (a 4D reduction) (23). Though products of this type have a good public health record, it is essential to adhere rigorously to recommended codes of practice concerning hygienic preparation and temperatures of cooking and refrigerated storage. Problems could arise, for example, if conditions during preparation allowed substantial growth before the heating step, especially if the heat process was relatively mild. Combined models that could predict both growth and inactivation would allow the relative safety margins of different processing regimens to be assessed.

Models for predicting growth of food-borne pathogens under a wide range of environmental conditions are now available (10, 12, 21). Validation tests have demonstrated that under constant temperature conditions, growth rates of microbes in food are close to those predicted by the models (20, 30). Models for predicting growth when temperature changes with time within the growth range have also been published (2, 11, 22, 31, 32).

The mathematical principles of thermal processing based on the traditional concepts of D and z values are well known (19, 24, 28), but there have been relatively few attempts to combine and validate models for growth and death of microbes. Although linking two models would appear to be a simple process, there are, in practice, several complicating factors. The main problem arises from the uncertainty in the behavior of microbes in the temperature zone around the growth-death boundary. If the model specifies that a change from a positive rate to a negative rate occurs at a discrete temperature, differences of a fraction of a degree can have a large effect on predicted behavior if the time spent around the transition point is appreciable. Microbial responses in this region are likely to be dependent on previous growth history and therefore somewhat unpredictable. The model behavior during the inactivation phase could thus exhibit extreme sensitivity to the initial conditions.

A further problem in combining two models is that of ensuring continuity at the joint boundary between the models. Van Impe et al. (31) linked a growth model described by a first-order differential equation to the thermal inactivation model of Bigelow (4), using an empirical function to describe the transition process.

Conventional thermal processing calculations assume that the heat resistance of microbes under changing conditions can be predicted from their behavior at static temperatures. This assumption is not true for vegetative cells of *Escherichia coli*, *Salmonella typhimurium*, and *L. monocytogenes*, whose resistance can increase during heating at rising temperatures (8, 9, 16–18, 25, 27, 30). Allowance for this increase in resistance must therefore be made in dynamic models.

In the work described here we derive a combined dynamic model for growth and subsequent thermal inactivation of *Brochothrix thermosphacta*, based on the approach described by Baranyi and Roberts (1) and Baranyi et al. (2). The model is tested by comparing the observed growth and death of *B. thermosphacta* in broth during heating at rising temperatures with behavior predicted by the model. The spoilage microbe *B. thermosphacta* was chosen as the test organism in developing the model because it is nonpathogenic and can therefore be used in validation studies with food conducted outside microbiology laboratories.

MATERIALS AND METHODS

Organism. *B. thermosphacta* MR 165 (NCFB 2891) was maintained on glass beads at −70°C. Working cultures were grown at 25°C on nutrient agar slopes and stored at 5°C.

Viable counts. Samples were diluted in Maximum Recovery Diluent (Oxoid catalog no. CM733), and 50-μl volumes were spread in duplicate on Tryptone Soya Agar (Oxoid catalog no. CM131). Viable numbers were estimated from colony counts after incubation for 48 h at 25°C.

Thermal inactivation in broth at constant temperatures. Cultures were grown at 25°C to an optical density at 680 nm of 0.2 in Tryptone Soya Broth (TSB; Oxoid catalog no. CM129) adjusted to pH 7 plus 0.5% NaCl (case 1) or in TSB adjusted to pH 5.9 plus 2% NaCl (case 2) (2). Samples were heated at 45, 48, 50, 52, and 55°C by one of the following three methods: (i) in sealed glass ampoules totally submerged in a stirred water bath; (ii) in the submerged coil apparatus described by Cole and Jones (7), or (iii) by addition of 1.0 ml of culture to 50 ml

* Corresponding author. Mailing address: Institute of Food Research, Reading Laboratory, Earley Gate, Whiteknights Rd., Reading RG6 6BZ, United Kingdom. Phone: 44 1734 357029. Fax: 44 1734 267917. Electronic mail address: BARANYI@BBSRC.AC.UK.

of preheated broth contained in a conical flask immersed up to its neck in a water bath. Samples were removed at various intervals for determination of viable counts.

Growth and inactivation in broth at changing temperatures. Cultures were grown for 16 to 18 h at 25°C as described by Baranyi et al. (2). The optical density of this culture was measured, and a volume sufficient to give an initial concentration of 10^3 cells per ml was added to 100 ml of TSB contained in a 250-ml bottle, which had been equilibrated to the desired temperature. Temperature ramps were created by a programmable water bath (RTE-2110P; Neslab Instruments, Inc.). Temperatures were recorded with a thermocouple attached to a logging device (Psion Organiser II with temperature logging module SF 10; Psion plc). The thermocouple was placed in 100 ml of distilled water in an identical bottle adjacent to the culture. Viable counts in the broth were determined at various intervals during the heating program.

Mathematical methods. A dynamic model for predicting growth and inactivation at rising temperatures was constructed in stages. Growth and inactivation data were obtained under constant temperature conditions. Curves were fitted to the natural logarithm of the measured bacterial concentrations, as detailed below, to estimate the respective maximum specific growth and death rates. Separate models for growth and inactivation were constructed to describe how these rates depended on temperature. The separate models were then joined together by means of a smoothing technique. A system of differential equations, solved numerically, predicted the growth of the organism under changing conditions.

(i) Fitting curves to isothermal growth or death rate data. In what follows, μ will denote the maximum specific rate of the growth or death curve (i.e., the steepest slope of the curve ln cell concentration versus time). With growth curves, μ is positive; with death curves, it is negative. By conventional terminology, doubling time equals ln 2/μ for growth curves and the D value equals $-\ln 10/\mu$ for death curves.

The thermal inactivation of microbes is conventionally described as conforming to pseudo-first-order kinetics, i.e., a plot of the logarithm of the surviving fraction against time gives a straight line. In our experiments the curves were often sigmoid or variants of sigmoid lacking the initial shoulder or tail regions (see Results).

Both the growth and inactivation curves were fitted by a special case of the model of Baranyi and Roberts (1) considering an inactivation curve as a mirror image of a growth curve. As shown by Baranyi et al. (2), that model, describing bacterial growth by a pair of differential equations, can also be used in cases in which temperature changes with time. For isothermal conditions, however, it has an explicit solution which can be expressed as

$$y(t) = y_0 + \mu A(t) - \frac{1}{m}\ln\left(1 + \frac{e^{m\mu A(t)} - 1}{e^{m(y_{max} - y_0)}}\right) \quad (1)$$

where

$$A(t) = t + \frac{1}{v}\ln(e^{-vt} + e^{-h_0} - e^{-vt-h_0}) \quad (2)$$

y_0 is the natural logarithm of the initial concentration, y_{max} is the natural logarithm of the cell concentration reached in stationary phase, μ is the maximum specific growth rate, v is a curvature parameter to characterize the transition to the exponential phase, m is a curvature parameter to characterize the transition from the exponential phase, and h_0 is the product of μ and the lag.

For curve fitting purposes, the inactivation curves were transformed into their mirror images by the following simple technique. (i) Denoting the natural logarithm of the measured cell concentrations of an inactivation curve by η_i (i = 0,. . .,$k - 1$), fix a value, say η_{fix}, which is greater than any η_i. Then, $\eta_i = \eta_{fix} - \eta_i$ (i = 0,. . ., $k - 1$), assigned to the same time values, will form a growth curve, a mirror image of the inactivation curve. (ii) Fit the obtained growth curve (y_0. . y_{k-1}) by the model of Baranyi and Roberts (1), where $y_0 = \eta_{fix} - \eta_0$ (η_0 is the natural logarithm of the cell concentration at the beginning of the inactivation curve); $y_{max} = \eta_{fix} - \eta_\infty$ (η_∞ is the natural logarithm of the cell concentration in the tail region of the inactivation curve); and μ is the maximum specific rate for the obtained growth curve, and so $-\mu$ is the maximum specific rate of the original inactivation curve.

As mentioned by Baranyi and Roberts (1), the last (logarithmic) terms in equations 1 and 2 are responsible for (i) the stationary-phase (or "tail," with death curves) and (ii) the lag phase (or "shoulder," with death curves), respectively.

Omitting one or both of those terms, the model allows curves to be fitted without shoulder and/or tail regions. According to this approach, a straight-line inactivation curve, for example, is a special case of the model. To choose the most appropriate curve to fit to the data, an F test was applied. Effectively, this decided whether it was worth introducing a transition to or from the exponential phase. If a transition-ensuring term was not omitted, then the values of the respective curvature parameter were fixed as $v = \mu$ and/or $m = 1$ accordingly (see the reasons given by Baranyi and Roberts [1]).

(ii) Rescaling the growth and death rates. The specific growth and death rates (μ values) are of different orders of magnitude and so are not easily representable in the same coordinate system. To overcome this problem, we rescaled this parameter by a useful, novel transformation designated the L transformation:

$$L(\mu) = \text{sign}(\mu) \cdot \ln(1 + |\mu|) \quad (3)$$

Here, sign(μ) is the so-called signum function:

$$\begin{matrix} 1, \text{ if } \mu > 0 \\ \text{sign}(\mu) = 0, \text{ if } \mu = 0 \\ -1, \text{ if } \mu < 0 \end{matrix} \quad (4)$$

The L transformation is continuous, invertible, and differentiable, leaving the sign of μ unchanged. $L(\mu)$ is close to μ if the absolute value of μ (denoted by $|\mu|$) is small but takes the (possibly negative) natural logarithm of $|\mu|$ if it is large. It provides a useful tool for rescaling the vertical axes of specific rate-versus-temperature plots such that for large μ values the plots appear to have a logarithmic scale, whereas for small μ values the scale appears linear. The specific rate, μ, is positive in the growth region, and therefore so is $L(\mu)$; it is negative in the death region ($\mu < 0$), and so is $L(\mu)$.

(iii) Constructing a smoothed combined model. Growth and death models were combined in a single smoothed model as follows: suppose that a growth model, $\mu = g(T)$, is given for $T \le T_1$ temperatures and a death model, $\mu = f(T)$, is given for $T \ge T_2$, where $T_1 \le T_2$. For the boundary temperature region (T_1,T_2), we model the bacterial growth by a zero model ($\mu = 0$) for the reasons described in the introduction.

To allow a smooth transition at the turning points T_1 and T_2, a combined model was constructed as follows: from the growth model, $g(T)$, construct a smoothed growth model, $G(T)$, according to the following rule: if $g(T)$, as well as its derivative, is zero at T_1, then leave $g(T)$ unchanged [$G(T) = g(T)$]. If this is not the case, introduce a so-called smoothing function:

$$S(T; T_0, w_0) = [1 - \exp(-w_0|T - T_0|)]^2 \quad (5)$$

where $w_0 > 0$ and apply it for $g(T)$:

$$G(T) = g(T) \cdot S(T; T_1, w_1) = g(T) \cdot \{1 - \exp[-w_1(T_1 - T)]\}^2 \quad (6)$$

for $T \le T_1$.

In the above expression, w_1 is a curvature parameter joining the growth model valid for $T \le T_1$ to the zero model which is assumed for the boundary region between growth and inactivation temperatures. For example, the square-root model for the entire growth range (26), rearranged to express the specific growth rate and not its square root, already contains the smoothing function. There, $g(T)$ is a parabolic function, $\sqrt{g(T)}$ being linear with temperature. However, the polynomial model of McClure et al. (20) needs to be completed by a smoothing function.

$F(T)$, the smoothed version of the $f(T)$ death model, can be constructed in a similar manner: if $f(T)$ and its derivative are zero at T_2, then leave $f(T)$ unchanged [$F(T) = f(T)$]; otherwise let $F(T)$ be defined as

$$F(T) = f(T) \cdot S(T; T_2, w_2) = f(T) \cdot \{1 - \exp[-w_2(T - T_2)]\}^2 \quad (7)$$

where $T \ge T_2$.

Just as above, w_2 is a curvature parameter joining the zero model of the (T_1,T_2) interval to the death model.

(iv) Predicting growth and death at rising temperatures. The dynamic model of Baranyi and Roberts (1) employs a pair of differential equations to describe microbial behavior under conditions that change with time. To predict combined growth and death curves, these differential equations must be solved numerically as described by Baranyi et al. (2).

The instantaneous specific growth rate at the time t, at rising temperatures, was calculated as

$$\begin{matrix} G(T) \text{ if } T \le T_1 \\ \mu(T) = 0 \text{ if } T_1 < T < T_2 + T_{shift} \\ F(T - T_{shift}) \text{ if } T_2 \le T \end{matrix} \quad (8)$$

where T is the actual temperature value at t. That is, we assume that in the growth phase the instantaneous specific rate corresponds to the actual temperature value but that in the inactivation phase it corresponds to a temperature value which is T_{shift} lower than the actual one. T_{shift} is an empirical correction term making the estimation of death rates fail-safe.

The results of the above-described procedure can be seen in Fig. 6 (see Results).

At a temperature profile, $T(t)$, increasing from the growth region to the inactivation region, the final model, rearranged from that of Baranyi and Roberts (1), can be written as

$$\frac{dy(t)}{dt} = \frac{1}{1 + e^{-Q(t)}}\mu[T(t)]\{1 - e^{m[y(t) - y_{max}]}\} \quad (9)$$

$$\frac{dQ(t)}{dt} = v[T(t)] \quad (10)$$

TABLE 1. Specific rates and their L-transformed values for growth and death of *B. thermosphacta*[a]

Case 1[b]			Case 2[c]		
Temp (°C)	μ (1/h)	$L(\mu)$	Temp (°C)	μ (1/h)	$L(\mu)$
2	0.156	0.145	2	0.060	0.058
2	0.111	0.105	2	0.056	0.054
5	0.230	0.207	5	0.137	0.128
5	0.205	0.186	5	0.149	0.139
10	0.411	0.344	10	0.285	0.251
10	0.345	0.296	10	0.209	0.190
20	0.849	0.615	20	0.462	0.380
20	0.836	0.608	20	0.481	0.393
25	1.324	0.843	25	0.541	0.432
25	1.430	0.888	25	0.897	0.640
30	0.800	0.588	30	0.560	0.445
30	0.905	0.644	30	0.600	0.470
45	−3.94	−1.60	45	−5.57	−1.88
45	−9.24	−2.33	45	−3.41	−1.48
45	−8.38	−2.24	45	−11.4	−2.52
45	−10.9	−2.48	48	−14.0	−2.71
45	−9.02	−2.30	48	−16.6	−2.87
45	−4.45	−1.70	50	−17.5	−2.92
45	−3.78	−1.57	50	−22.6	−3.16
48	−16.2	−2.85	52	−75.4	−4.34
48	−11.6	−2.53	52	−57.1	−4.06
48	−15.0	−2.77	55	−257	−5.55
50	−26.5	−3.31	55	−145	−4.99
50	−23.7	−3.21	55	−150	−5.02
50	−25.0	−3.26			
52	−59.8	−4.11			
55	−243	−5.50			
55	−261	−5.57			

[a] Data for temperatures below 30°C are those of Baranyi et al (2).
[b] Environmental conditions: pH 7 and 0.5% NaCl.
[c] Environmental conditions: pH 5.9 and 2% NaCl.

with the initial values

$$y(0) = y_0 \quad (11)$$

$$Q(0) = -\ln(e^{h_0} - 1) \quad (12)$$

The so-called initial value problem, represented by equations 9 to 12, with the simplifying assumptions that $m = 1$ and

$$v[T(t)] = \mu[T(t)] \quad (13)$$

was solved numerically to give predictions for bacterial curves at temperatures increasing with time. Here, y_0 is the initial cell concentration and h_0 quantifies the suitability of the cells to the postinoculation environment. The value of h_0, which is also the product of the lag and the maximum specific growth rate in isothermal growth curves, was taken to be constant, as estimated by Baranyi et al. (2). The function $\mu[T(t)]$ is defined by the given temperature profile and the growth and death rate models (functions g and f) determined under isothermal conditions and combined into a smooth, continuous function by equations 6, 7, and 8. Note that for constant temperature, the solution of the initial value problem presented above is given by equations 1 and 2 as discussed in more detail in Baranyi and Roberts (1).

RESULTS

Growth model. The specific growth rates of *B. thermosphacta* in broth at pH 7 containing 0.5% NaCl (case 1) and in broth at pH 5.9 containing 2% NaCl (case 2) are partly taken from Baranyi et al. (2) (below 30°C) and partly estimated from new experiments as reported below (Table 1). The temperature dependence of growth (function g in the section "Mathematical methods" above) was described by the square-root model of Ratkowsky et al. (26), of the form

$$\sqrt{\mu} = \sqrt{g(T)} = b(T - T_{\min})\{1 - \exp[-w_1(T_1 - T)]\} \quad (14)$$

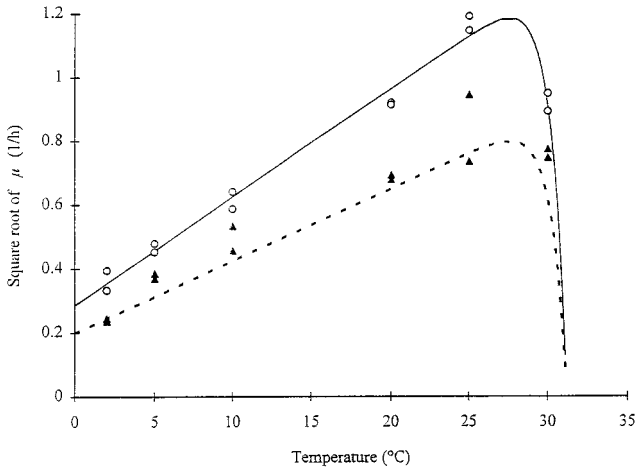

FIG. 1. Specific growth rates (μ) of *B. thermosphacta* fitted by the square-root model. Open circles with continuous line, specific growth rates under conditions of case 1 (pH 7; 0.5% NaCl); filled triangles with broken line, specific growth rates under conditions of case 2 (pH 5.9; 2% NaCl). T_1, the upper temperature of the growth region (lower limit of the boundary temperature region), is practically identical for case 1 and case 2.

where b, $T_{\min}$, w_1, and T_1 are model parameters.

Fitted curves and parameters are shown in Fig. 1 and 2, respectively. The slope parameter b_1 was different for the different growth conditions (cases 1 and 2), but there were no significant differences between the temperature parameters $T_{\min}$ and T_1.

Inactivation kinetics. Semilogarithmic plots of survival data were often sigmoid or otherwise nonlinear. Examples of inactivation curves fitted to data as described in Materials and Methods are shown in Fig. 3.

To investigate whether the nonlinear kinetics were caused by the heating method, we compared survivor curves obtained from the same cell suspension heated in (i) submerged ampoules, (ii) a submerged coil apparatus, and (iii) a flask immersed up to its neck in a water bath. Nonlinear curves were obtained by all methods and confirmed by application of the F test, suggesting that the phenomenon was not a methodological artifact (data not shown). There was no consistent pattern to the particular shape of curve obtained under different heating conditions, although the type shown in Fig. 3d was more common at higher temperatures.

If curves are genuinely sigmoid, it implies the existence of a more resistant fraction in the population or a change in resistance during heating. The number of organisms that compose the tail is small and near the detection limit for plate counts. It is therefore difficult to obtain reliable data for the rate of inactivation in this region. We attempted to obtain more pre-

	c_1	c_2	T_2	T_{shift}
Case 1 and 2	0.31	0.138	36.7	3.14

	b_1	T_{min}	T_1	b_2	T_{ref}
Case 1	0.034	-8.4	31.1	0.34	39.9
Case 2	0.023	-8.8	31.2	0.35	40

FIG. 2. Estimated coefficients for the combined model.

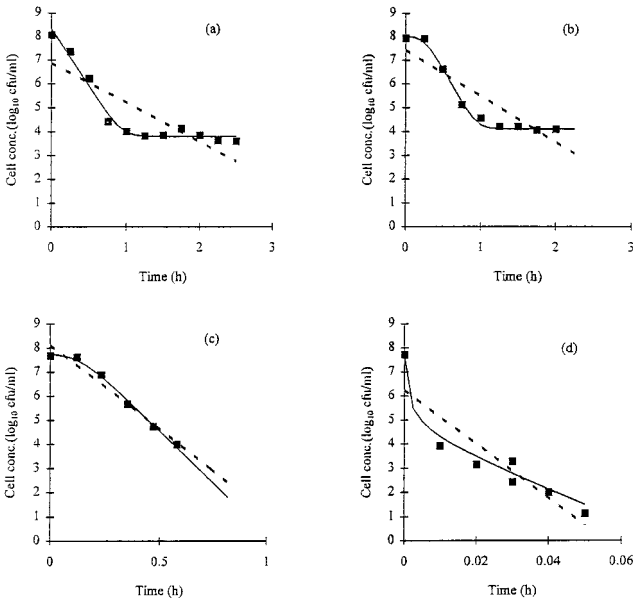

FIG. 3. Thermal inactivation curves for *B. thermosphacta* at 45°C, pH 7, and 0.5% NaCl (example of a curve without a shoulder but with a tail) (a); at 45°C, pH 7, and 0.5% NaCl (example of a curve with a shoulder and with a tail) (b); at 48°C, pH 5.9, and 2% NaCl (example of a curve with a shoulder and without a tail) (c); and at 55°C, pH 5.9, and 2% NaCl (example of a curve with a sudden initial decrease followed by an exponential phase) (d). The curves were fitted by the mirror image of the model of Baranyi and Roberts (1) (continuous line), as well as by a simple linear function (broken line). Note the different time scales of the plots. conc., concentration.

cise data by heating suspensions that had been concentrated by centrifugation and resuspension, but this procedure altered both the kinetics of inactivation and the fraction of organisms in the tail in an unpredictable way (data not shown).

For many curves, a straight line was not the best fit to the data (Fig. 3). However, even though a better fit could be obtained with a sigmoid curve, the rate μ so obtained applied only to that part of the curve in which inactivation occurred most rapidly. This rate was not representative of the whole inactivation process and would overestimate the lethality of a heat treatment. For this reason, approximate but generally fail-safe estimates of μ were obtained from straight-line fits (Fig. 3).

Inactivation model. The inactivation model is analogous to the conventional *D* and *z* model for thermal inactivation. The assumption that the *z* value is constant is equivalent to the assumption that $\ln(-\mu)$ depends linearly on temperature (the function *f* in the section "Mathematical methods"), i.e.,

$$\ln(-\mu) = \ln[-f(T)] = b_2(T - T_{\text{ref}}) \qquad (15)$$

where b_2 and T_{ref} are model parameters.

From this, it follows that $z = \ln 10/b_2$. Inactivation rates determined in this work are listed in Table 1. There were no significant differences between cases 1 and 2 in terms of the estimated b_2 and T_{ref} parameters (Fig. 2 and 4).

Establishing the boundary region between growth and inactivation temperatures. The model described above does not allow a lower temperature boundary for the inactivation region to be established, because $\ln(-\mu)$ cannot be zero. The *L* transformation (see Materials and Methods) proved useful in resolving this problem. We fitted all the $L(\mu)$ values (from both case 1 and case 2), by the function

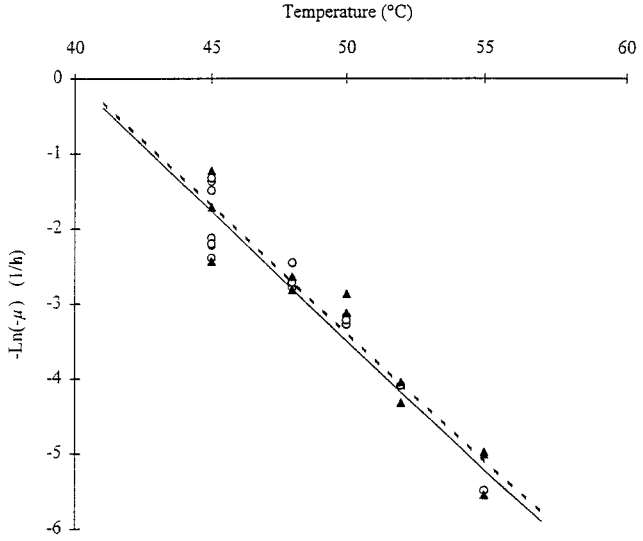

FIG. 4. Modelling the specific death rates ($\mu < 0$) of *B. thermosphacta* in terms of temperature. The assumption that the *z* value of the organism is constant is equivalent to a linear model for the $\ln(-\mu)$-versus-temperature relation. The legend is as for Fig. 1.

$$L(\mu) = -c_1(T - T_2)/\{1 + \exp[-c_2(T - T_2)]\} \qquad (16)$$

with three parameters, c_1, c_2, and T_2, being fitted (Fig. 5). The estimated values are plotted and tabulated in Fig. 2 and 5, respectively. The lower boundary of inactivation temperatures, T_2, is set equal to that temperature at which $L(\mu) = 0$, i.e., at which $\mu = 0$. The corresponding upper temperature limit for growth was defined, from the growth model, as the temperature at which $\mu = 0$. Because the boundary temperatures were practically identical for both case 1 and case 2, the (T_1,T_2) interval was estimated as $T_1 = 31.2$°C and $T_2 = 36.7$°C for both cases. In the combined model, it is assumed that growth and death rates in this region are zero.

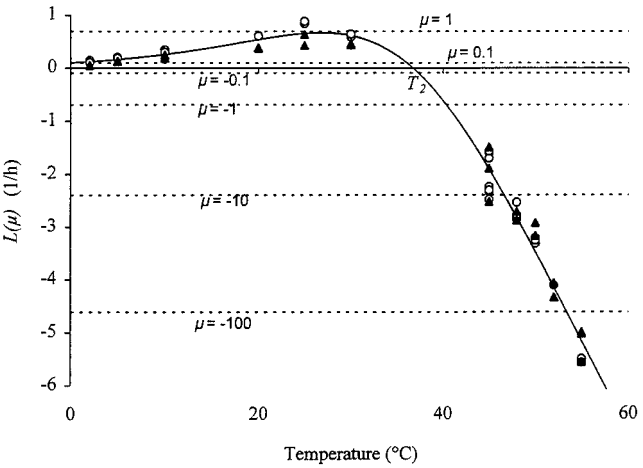

FIG. 5. Fitting the *L* values of the specific growth and death rates of *B. thermosphacta* together for case 1 (pH 7; 0.5% NaCl) and case 2 (pH 5.9; 2% NaCl). Rescaling the μ values allowed specific growth and death rates to be represented on the same graph; if $|\mu|$ is small, then $L(\mu) \approx \mu$; otherwise, $L(\mu) \approx \ln \mu$. The zero point of the fitted function gives an estimation for the upper limit, T_2, of the boundary temperature region (lower limit of inactivation temperatures).

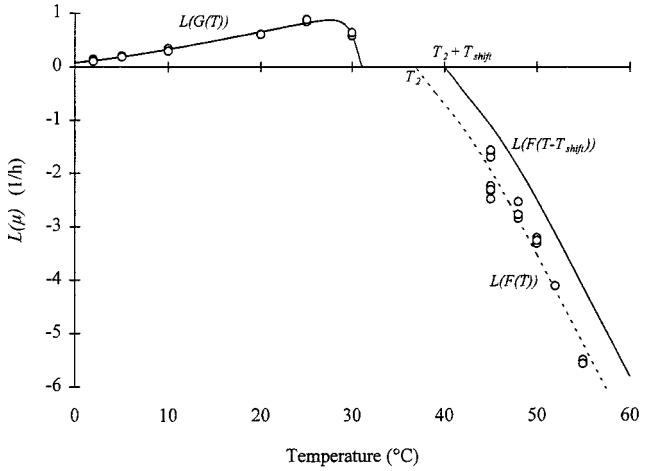

FIG. 6. The final combined model for the temperature dependence of the specific growth-death rate of *B. thermosphacta* for conditions of case 1 (pH 7; 0.5% NaCl). The growth and death models are joined to the boundary temperature region (where growth and death rates are assumed to be zero) by an empirical smoothing function. The continuous line indicates the model with the T_{shift} = 3.14°C correction term. The broken line indicates the inactivation model when the increase in resistance of the cells during the slow heating is not taken into account (T_{shift} = 0).

Combining the growth and inactivation models. Having established the temperatures delineating the boundary temperature region, we joined the growth and death models by using the smoothing technique described in Materials and Methods. Because the data were insufficient to establish the curvature parameters w_1 and w_2, the values of these parameters were fixed empirically at 1.

For the functions $G(T)$ and $F(T)$, described by equations 6 and 7, the following equations were obtained:

$$G(T) = [b_1(T - T_{min})]^2 \cdot \{1 - \exp[-w_1(T_1 - T)]\}^2 \quad (17)$$

for $T \leq T_1$ and

$$F(T) = -\exp[b_2(T - T_{ref})] \cdot \{1 - \exp[-w_2(T - T_2)]\}^2 \quad (18)$$

for $T \geq T_2 + T_{shift}$.

In this combined model, the boundary temperature region is joined by a smooth transition to the growth and death regions. When cases 1 and 2 were compared, significant difference was found in the estimated values of the parameter b_1 only (b_1 = 0.034 and 0.023, respectively). Therefore, the other parameters were taken, in both cases, to be as follows: $T_{min} = -8.6$, T_1 = 31.2, b_2 = 0.35, T_{ref} = 40, and T_2 = 36.7. The model is demonstrated in Fig. 6.

Compensation for heat shock-induced thermotolerance. Initial experiments revealed that the model overestimated the rate of inactivation during heating at rising temperatures, i.e., the cells were more resistant than predicted from isothermal data. To compensate for this increased resistance, a correction term, T_{shift}, was introduced (see equation 8). To estimate a value for T_{shift}, unpublished data of Mackey and Derrick that showed that the maximum increase in resistance of *S. typhimurium* or *L. monocytogenes* following heat shock corresponded to an approximately threefold increase in D value were taken into account. Calculating with $D_{corr} = b_2 = 0.35$ (Fig. 2), T_{shift} can be estimated by

$$T_{shift} \approx \ln D_{corr}/b_2 = \ln 3/0.35 = 3.14\ (°C) \quad (19)$$

That is, we assume that when the transition from growth phase to inactivation phase is relatively slow, the inactivation in fact begins only at the temperature $T_2 + T_{shift}$. For a higher temperature, the instantaneous specific death rate corresponds to a μ value measured in isothermal experiments at a temperature which is T_{shift} lower than the actual instantaneous temperature.

Applying the formula described in Materials and Methods, the final formula for the specific rate in the inactivation region is:

$$\mu = F(T - T_{shift}) \quad (20)$$

for $T \geq T_2 + T_{shift}$. The difference between $F(T)$ and $F(T - T_{shift})$ is shown in Fig. 5.

Validation of the combined growth-death model in broth. Predictions of the combined growth and death model were compared with changes in viable numbers experimentally observed as temperatures increased through the growth range into the inactivation range.

Results for growth and subsequent inactivation in broth during a linear increase in temperature between 10 and 50°C over 35 h (pH 5.9; 2% NaCl) are shown in Fig. 7. As in the paper of Baranyi et al. (2), two curves were predicted, one with no lag phase and one with a typical lag phase. The measured log counts were in this case closest to the predicted curve for no lag. Note that both predicted curves include the T_{shift} correction term.

A similar validation experiment was done in broth at pH 7 containing 0.5% NaCl, with temperature changing linearly from 25 to 59°C in 24 h. Beside the predicted curves as described above, Fig. 8 also includes a predicted curve with T_{shift} = 0, showing that omission of the correction factor would result in an overestimation of lethality.

DISCUSSION

Inactivation rates. Several problems associated with constructing a combined model for growth and thermal inactivation were outlined in the introduction. In addition to these, it emerged that experimentally observed inactivation rates for *B.*

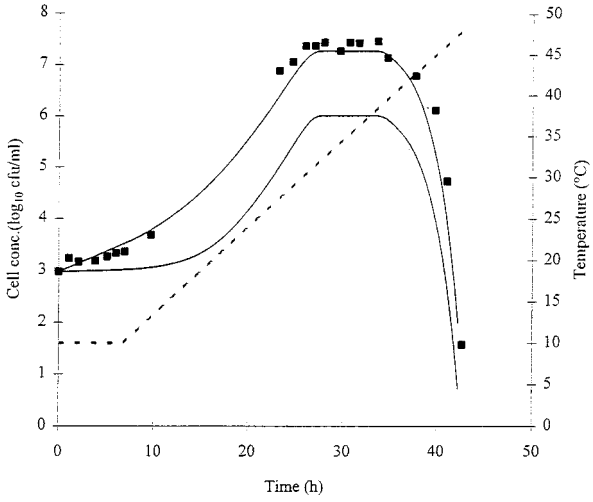

FIG. 7. Predicted (continuous lines) and measured (filled squares) viable counts of *B. thermosphacta* grown and then subsequently inactivated in TSB at pH 5.9 and 2% NaCl, with slowly increasing temperature (T_{shift} = 3.14°C). Broken line, temperature profile; upper solid line, predicted curve with no lag; lower solid line, predicted curve with typical lag determined from isothermal data. conc., concentration.

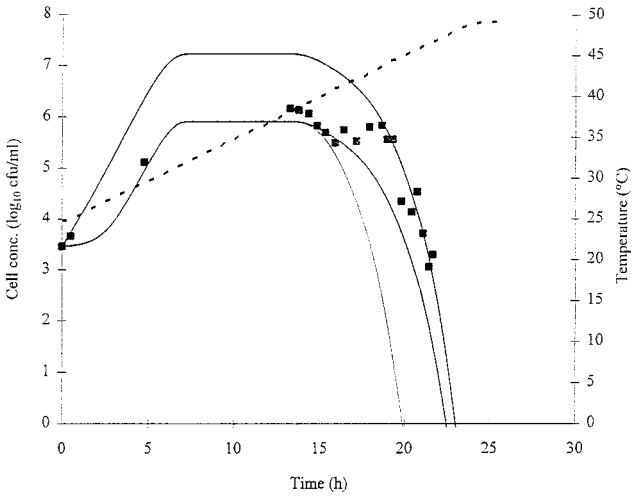

FIG. 8. Predicted and measured viable counts of *B. thermosphacta* grown and then subsequently inactivated in TSB at pH 7 and 0.5% NaCl with slowly increasing temperatures. The legend is as for Fig. 7. The thin continuous line in the inactivation phase indicates the predicted curve with no allowance for an increase in resistance during slow heating ($T_{shift} = 0$).

thermosphacta deviated from the first-order behavior assumed in conventional models based on *D* and *z* values. Similar nonlinear curves have been reported for thermal inactivation of other microbes (5, 13, 27). Whether such nonlinear curves represent true inactivation rates or are methodological artifacts remains controversial. Since we obtained sigmoid or other nonlinear curves by more than one technique, it is necessary to suppose that all the methods, including the use of totally submerged sealed glass ampoules, induced similar artifacts. In view of the variety of curves observed in different experiments and the way in which attempts to concentrate cells affected the kinetics, it seems more reasonable to suppose that the observed kinetics are real but highly dependent on the physiological state of the cells. However, until the physiological basis of tailing is fully understood, it is impossible to assess its practical significance.

Others who have reported sigmoid inactivation curves have calculated rates with the Gompertz equation (3). The rates so obtained are derived from the most rapid phase of inactivation and, if used in process calculations, would overestimate the degree of inactivation if appreciable shoulder or tail regions exist. An alternative, "vitalistic" model for describing nonlinear inactivation kinetics was described by Cole et al. (6). In this approach, the use of the logistic function with log heating time allowed the development of an accurate predictive model.

Because the shapes of survivor curves of *B. thermosphacta* were variable, we chose to take the rate based on a straight-line fit. For a sigmoid curve this would overestimate the rate during the initial phase of inactivation but would underestimate the rate during the latter phase. We believe this simple approach to be appropriate because (i) inactivation rates increase exponentially with temperature so that small deviations from the actual order of death at any particular temperature become insignificant when the total thermal process, covering a wide range of temperatures, is considered and (ii) our approach would yield unsafe predictions only if the tail region of the curve were unduly prolonged. We have no evidence that this was so, but the thermal properties of the last surviving cells in a heated population require clarification.

Many processes designed to inactivate vegetative microbes are based on reducing viable numbers by factors of 10^5 to 10^7, i.e., by 5 to 7 $\log_{10}$ units (15). Since the tail portion of the curve often comprised a fraction equal to only 10^{-5} to 10^{-7}, it is possible to achieve these reductions within the other 99.999 to 99.99999% of the population, i.e., rates calculated without reference to a tail would not prejudice the safety of processes based on these levels of reduction.

Construction of a combined model. A general problem associated with joining different models, viz., that of dealing with behavior at the transition region, was solved in our combined growth-death model by considering the specific rate to be zero in the boundary temperature region. This simple approach was no less accurate than other, more complex, methods.

An appropriate upper temperature limit for the growth model was obtained simply by extrapolating the applied square-root growth model to the temperature at which the growth rate would be zero. It is not possible to extrapolate the inactivation model to a zero rate in a similar manner, because the logarithmic relationship between rate and temperature means that the zero rate is approached asymptotically. To overcome this problem, a novel rescaling procedure (the *L* transformation) that gave an objective method to define the lower temperature of inactivation was employed. To prevent abrupt discontinuities at the limits of the two models, so defined, a smoothing function was applied. Its role, as its name indicates, is simply to smooth the transition to and from the boundary temperature region.

The initial validation of the combined model revealed that *B. thermosphacta* was more resistant when heated at rising temperatures than predicted from isothermal data. We assume that this effect is caused by heat shock-induced thermotolerance as demonstrated for other organisms (8, 9, 16–18, 25, 27, 30). The degree of increased resistance depends on the heating rate (17, 27). If the relationship between heating rate and increased resistance were known, it would be possible to construct more precise models for inactivation at rising temperatures. However, a simpler, fail-safe approach is to assume the maximum possible increase. Quantitative data for different organisms are scarce, but indications are that the maximum increase corresponds to an approximately threefold increase in *D* value. For *B. thermosphacta*, this means that the instantaneous specific death rates of organisms heated up slowly correspond to rates measured in isothermal experiments at temperatures about 3°C lower. When an empirical shift term (T_{shift}) correcting for the effect of increased resistance was included in the model, the predictions were satisfactory. The effect of increased resistance during slow heating may be important in products given marginal heat processes.

The combined model described here incorporated several new mathematical features that overcame the inherent problems associated with combining separate growth and death models. Validation studies showed that the model accurately predicted growth and inactivation of *B. thermosphacta* in broth during heating at rising temperatures. The approaches developed in this work will be applicable to other food-borne organisms, allowing the relative safety margins of different preparation and processing regimens to be assessed.

ACKNOWLEDGMENTS

This work was supported by European Community FLAIR (Food Linked Agro-Industrial Research) grant AGRF-DT91-0047 and by the U.K. Office of Science and Technology via the Biotechnology and Biological Sciences Research Council.

REFERENCES

1. **Baranyi, J., and T. A. Roberts.** 1994. A dynamic approach to predicting bacterial growth in food. Int. J. Food Microbiol. **23:**277–294.

2. **Baranyi, J., T. P. Robinson, A. Kaloti, and B. M. Mackey.** 1995. Predicting growth of *Brochothrix thermosphacta* at changing temperature. Int. J. Food Microbiol. **24:**61–75.
3. **Bhaduri, S., P. W. Smith, S. Palumbo, C. O. Turner-Jones, J. L. Smith, B. S. Marmer, R. L. Buchanan, L. L. Zaika, and A. C. Williams.** 1991. Thermal destruction of *Listeria monocytogenes* in liver sausage. Food Microbiol. **8:** 75–78.
4. **Bigelow, W. D.** 1921. The logarithmic nature of thermal death time curves. J. Infect. Dis. **29:**528.
5. **Cerf, O.** 1977. Tailing of survival curves of bacterial spores. J. Appl. Bacteriol. **42:**1–19. (Review.)
6. **Cole, M. B., K. W. Davies, G. Munro, C. D. Holyoak, and D. Kilsby.** 1993. A vitalistic model to describe the thermal inactivation of *Listeria monocytogenes*. J. Ind. Microbiol. **12:**232–239.
7. **Cole, M. B., and M. V. Jones.** 1990. A submerged coil apparatus for investigating thermal inactivation of microorganisms. Lett. Appl. Microbiol. **11:** 233–235.
8. **Farber, J. M., and B. E. Brown.** 1990. Effect of prior heat shock on heat resistance of *Listeria monocytogenes* in meat. Appl. Environ. Microbiol. **56:** 1584–1587.
9. **Fedio, W. M., and H. Jackson.** 1989. Effect of tempering on the heat resistance of *Listeria monocytogenes*. Lett. Appl. Microbiol. **9:**157–160.
10. **Food MicroModel, version 1.** 1994. Food Micromodel Ltd., Leatherhead, Surrey, United Kingdom.
11. **Fu, B., P. S. Taoukis, and T. Labuza.** 1991. Predictive microbiology for monitoring spoilage of dairy products with time-temperature integrators. J. Food Sci. **56:**1209–1215.
12. **Hills, B. P., and K. M. Wright.** 1995. A new model for bacterial growth in heterogeneous systems. J. Theor. Biol. **168:**39–41.
13. **King, A. D., H. G. Bayne, and G. Alderton.** 1979. Nonlogarithmic death rate calculations for *Byssochlamys fulva* and other organisms. Appl. Environ. Microbiol. **37:**596–600.
14. **Lund, B. M., and S. H. W. Notermans.** 1992. Potential hazards associated with REPFEDS, p. 279–303. *In* H. W. Hauschild and K. L. Dodds (ed.), *Clostridium botulinum* ecology and control in foods. Marcel Dekker, Inc., New York.
15. **Mackey, B. M., and N. Bratchell.** 1989. The heat resistance of *Listeria monocytogenes*. Lett. Appl. Microbiol. **9:**89–94. (Review.)
16. **Mackey, B. M., and C. M. Derrick.** 1986. Elevation of the heat resistance of *Salmonella typhimurium* by sublethal heat shock. J. Appl. Bacteriol. **61:** 389–393.
17. **Mackey, B. M., and C. M. Derrick.** 1987. Changes in heat resistance of *Salmonella typhimurium* during heating at rising temperatures. Lett. Appl. Microbiol. **4:**13–16.
18. **Mackey, B. M., and C. M. Derrick.** 1987. The effect of prior heat shock on the thermoresistance of *Salmonella thompson* in foods. Lett. Appl. Microbiol. **5:**115–118.

18a. **Mackey, B. M., and C. M. Derrick.** Unpublished data.

19. **Matsuda, N., M. Komaki, and K. Matsunawa.** 1983. Thermal death characteristics of spores of *Clostridium botulinum* 62A and *Bacillus stearothermophilus* subjected to programmed heat treatment, p. 51–62. *In* T. Motohiro and K. Hayakawa (ed.), Heat sterilisation of food. Koseisha-Koseikaku Co. Ltd., Tokyo.
20. **McClure, P. J., J. Baranyi, E. Boogard, T. M. Kelly, and T. A. Roberts.** 1993. A predictive model for the combined effect of pH, sodium chloride and storage temperature on the growth of *Brochothrix thermosphacta*. Int. J. Food Microbiol. **19:**161–178.
21. **McMeekin, T. A., J. N. Olley, T. Ross, and D. A. Ratkowsky.** 1993. Predictive microbiology. John Wiley & Sons Ltd., Chichester, United Kingdom.
22. **Mitchell, G. A., T. F. Brockelhurst, R. Parker, and A. C. Smith.** 1994. The effect of transient temperatures on the growth of *Salmonella typhimurium* LT2. I. Cycling within the growth range. J. Appl. Bacteriol. **77:**113–119.
23. **National Advisory Committee on Microbiological Criteria for Foods.** 1990. Recommendations for refrigerated foods containing cooked, uncured meat or poultry products that are packed for extended, refrigerated shelf life and that are ready-to-eat or prepared with little or no additional heat treatment. Adopted January 1990. National Advisory Committee on Microbiological Criteria for Foods, Washington, D.C.
24. **Patashnik, M.** 1953. A simplified method for thermal process evaluation. Food Technol. **7:**1–6.
25. **Quintavalla, S., and M. Campanini.** 1991. Effect of rising temperature on the heat resistance of *Listeria monocytogenes* in meat emulsion. Lett. Appl. Microbiol. **12:**184–187.
26. **Ratkowsky, D. A., R. K. Lowry, T. A. McMeekin, A. N. Stokes, and R. E. Chandler.** 1983. Model for bacterial culture growth rate throughout the entire biokinetic temperature range. J. Bacteriol. **154:**1222–1226.
27. **Resnik, S. L., and J. Chirife.** 1988. Proposed theoretical a_w values at various temperatures for selected solutions to be used as reference sources in the range of microbial growth. J. Food Prot. **51:**419–423.
28. **Stephens, P. J., M. B. Cole, and M. V. Jones.** 1994. Effect of heating rate on the thermal inactivation of *Listeria monocytogenes*. J. Appl. Bacteriol. **77:** 702–708.
29. **Stumbo, C. R.** 1973. Thermobacteriology in food processing. Academic Press, New York.
30. **Sutherland, J. P., A. J. Bayliss, and T. A. Roberts.** 1993. Predictive modelling of growth of *Staphylococcus aureus*: the effects of temperature, pH and sodium chloride. Int. J. Food Microbiol. **21:**217–236.
31. **Tsuchido, T., M. Hayashi, M. Takano, and I. Shibasaki.** 1982. Alteration of thermal resistance of microorganisms in a non-isothermal heating process. J. Antibact. Antifung. Agents **10:**105–109.
32. **Van Impe, J. F., B. M. Nicolai, T. Martens, J. Baerdemaeker, and J. Vandewalle.** 1992. Dynamic mathematical model to predict microbial growth and inactivation during food processing. Appl. Environ. Microbiol. **58:**2901–2909.
33. **Zwietering, M. H., H. G. A. M. Cuppers, J. C. De Wit, and K. Van't Reit.** 1994. Modeling bacterial growth with shifts in temperature. Appl. Environ. Microbiol. **60:**204–213.